

Effects of Diffusion of Hydrogen and Oxygen on Electrical Properties of Amorphous Oxide Semiconductor, In-Ga-Zn-O

To cite this article: Kenji Nomura *et al* 2013 *ECS J. Solid State Sci. Technol.* **2** P5

View the [article online](#) for updates and enhancements.

You may also like

- [Roles of Hydrogen in Amorphous Oxide Semiconductor In-Ga-Zn-O: Comparison of Conventional and Ultra-High-Vacuum Sputtering](#)

Takaya Miyase, Ken Watanabe, Isao Sakaguchi *et al.*

- [\(Invited\) Depth Analysis of Near Valence Band Maximum Defect States in Amorphous Oxide Semiconductors: Amorphous in-Ga-Zn-O](#)

Keisuke Ide, Masato Ota, Takayoshi Katase *et al.*

- [\(Invited\) Roles of Hydrogen in Amorphous Oxide Semiconductor](#)

Toshio Kamiya and Hideo Hosono



Your Lab in a Box!

The PAT-Tester-i-16: All you need for Battery Material Testing.

- ✓ All-in-One Solution with integrated Temperature Chamber!
- ✓ Cableless Connection for Battery Test Cells!
- ✓ Fully featured Multichannel Potentiostat / Galvanostat / EIS!

www.el-cell.com +49 40 79012-734 sales@el-cell.com


electrochemical test equipment





Effects of Diffusion of Hydrogen and Oxygen on Electrical Properties of Amorphous Oxide Semiconductor, In-Ga-Zn-O

Kenji Nomura,^{a,z} Toshio Kamiya,^b and Hideo Hosono^{a,b}

^aFrontier Research Center, Tokyo Institute of Technology, Midori-ku, Yokohama 226-8503, Japan

^bMaterials and Structures Laboratory, Tokyo Institute of Technology, Midori-ku, Yokohama 226-8503, Japan

We found that device-quality thin films of amorphous oxide semiconductor, a-In-Ga-Zn-O, unintentionally include high-density hydrogens over 10^{20} cm^{-3} but the electron concentration remains low at $\sim 10^{15} \text{ cm}^{-3}$ in as-deposited states. The hydrogens exist in the form of hydroxyl group $-\text{OH}$, but most of them are inactive as an electron donor, which is explained by charge compensation due to incorporation of excess oxygens. Although their diffusions are fast compared with those in crystalline ZnO, but oxygen can diffuse only 20 nm even at 400°C . Hydrogen diffusion is much faster, and easily hydrogenizes a thin channel of a thin-film transistor. © 2012 The Electrochemical Society. [DOI: 10.1149/2.011301jss] All rights reserved.

Manuscript submitted May 31, 2012; revised manuscript received October 12, 2012. Published November 6, 2012.

Transparent amorphous oxide semiconductors (TAOSs) represented by amorphous In-Ga-Zn-O (a-IGZO) are expected for thin-film transistors (TFTs) in next-generation flat-panel displays (FPDs) because of their large electron mobilities of $> 10 \text{ cm}^2(\text{Vs})^{-1}$ and low-temperature processability.¹ Therefore, panel manufacturers have conducted intensive development research and produced many prototype FPDs using a-IGZO TFTs as switching/driving TFTs.²

It is known that hydrogen has a crucial role in semiconductors, e.g., to passivate dangling bonds in amorphous Si and to form shallow donor states in several oxide semiconductors including ZnO and a-IGZO.^{3,4} Also oxygen is important in oxide semiconductors because oxygen deficiency is related closely to formation of donor states and electron traps. For a-IGZO, off-stoichiometric oxygens including oxygen deficiency and excess oxygen play a crucial role in formations of shallow donor states and subgap trap states, which largely affect the TFT characteristics.⁵

In a previous work, we detected rather high-density ($> 10^{19} \text{ cm}^{-3}$) desorption of hydrogen-related species such as H_2O and H_2 from room-temperature- (RT) deposited a-IGZO films by thermal gas desorption spectroscopy (TDS) measurements.⁶ However, the free carrier density (N_e) of the films were as low as 10^{15} cm^{-3} , which was unexpected because hydrogen is considered to work as an electron donor in a-IGZO by ionized to H^+ and forming $-\text{OH}$ bonds.⁴ Moreover, we also found that a-IGZO can incorporate weakly-bonded excess oxygens, which form electron traps and cause large degradation of TFT characteristics,⁵ while the desorption of them is thought to reduce the electron traps and release the free electrons. Therefore, to understand chemical bonding states, diffusion of hydrogen and oxygen in a-IGZO is of great importance to control and further improve the electrical property and long-term stability of a-IGZO devices.

In this study, we investigated the diffusion of hydrogen and oxygen in a-IGZO (In : Ga : Zn \sim 1:1:1 in atomic ratio) thin films in relation to electrical properties. As a result, we consider that hydrogens form $-\text{OH}$ bonds and work as electron donors, but most of the free electrons are compensated by excess oxygens.

A-IGZO films with 80–100 nm in thickness were prepared on thermally-oxidized SiO_2 ($t \sim 150 \text{ nm}$) / n^+ -Si wafers by pulsed laser deposition (PLD) at RT. Oxygen pressure (P_{O_2}) was fixed at 6.7 Pa during the deposition. The chemical composition depth profiles were measured by secondary ion mass spectrometry (SIMS) with a Cs^+ primary ion source and detection of negative secondary ions, and also by Rutherford backscattering spectrometry / hydrogen forward scattering spectrometry (RBS/HFS) with He^{2+} ion beam. Attenuated total reflection-Fourier transform infrared spectroscopy (ATR-FTIR) and microscopic laser Raman spectroscopy were used to investigate the chemical bonding state of the hydrogen impurity. Isotope diffusion experiments were performed by a gas-solid technique using the isotope

deuterium (^2D) and ^{18}O as hydrogen and oxygen tracers, respectively. For ^2D diffusion, the as-deposited films were subjected to thermal annealing in a 5%- D_2 /95%- N_2 atmosphere, while ^{18}O diffusion was performed in a sealed silica tube fully filled by a 98%- ^{18}O gas. The diffusion temperature (T_{ann}) was varied from 100 to 400°C , and the diffusion duration was fixed to 1 hour.

We firstly analyzed the content and the chemical states of hydrogen in the as-deposited a-IGZO films with N_e of $\sim 10^{15} \text{ cm}^{-3}$. Figure 1a and 1b show the chemical composition depth profiles of hydrogen ([H]) obtained by SIMS and RBS/HFS. Both revealed that the a-IGZO films contained hydrogens at the high densities of $[\text{H}] \sim 3\text{--}4 \times 10^{20}$ (SIMS) and $\sim 2 \times 10^{20} \text{ cm}^{-3}$ (HFS). Although the constituent elements of a-IGZO such as In, Ga, Zn, and O homogeneously distributes in the whole region of the films, the [H] clearly decreases toward the film surface, indicating out-diffusion of the internal H during the film deposition. The source of the hydrogen is not clear yet but residual H-containing species in the deposition chamber and the sputtering target are candidates.

Figures 1c and 1d show the ATR-FTIR and Raman spectra for the as-deposited a-IGZO films, respectively. For the ATR-FTIR spectra, two broad absorptions from the film are observed around 661.8 cm^{-1} ($^{\text{v}}(\text{In,Ga,Zn})\text{-O}^{\text{v}}$ in Fig. 1c) and 3240 cm^{-1} with the band width of 600 cm^{-1} ($^{\text{v}}\text{-OH}^{\text{v}}$ in a magnified view, inset to Fig. 1c), which are attributed to metal (In, Ga and Zn)-oxygen ($M\text{-O}$) bond stretching vibrations and hydroxyl ($-\text{OH}$) bond stretching vibrations, respectively. The very weak and broad absorption of $-\text{OH}$ exclude the possibility that H_2O molecule is existed in a-IGZO because H_2O molecules exhibit a sharp absorption band even in a solid (it is reported that the IR band for H_2O molecules in SiO_2 appears at $\sim 3270 \text{ cm}^{-1}$ with the small band width of $\sim 100 \text{ cm}^{-1}$ ⁷). The Raman spectra also show broad $-\text{OH}$ bonds at 3480 cm^{-1} ($^{\text{v}}\text{1}^{\text{v}}$ in inset to Fig. 1d) with Raman bands attributed to $M\text{-O}$ vibrations (182, 310, and 600 cm^{-1} , denoted 'a-IGZO' in Fig. 1d). No Raman band related to H_2 molecules (Raman shift $\sim 4160 \text{ cm}^{-1}$) was observed (we confirmed that $\sim 2 \times 10^{18} \text{ cm}^{-3}$ of H_2 should be detectable by this measurement condition). Therefore, we concluded that as-deposited a-IGZO contained hydrogens at $[\text{H}] \gg 10^{20} \text{ cm}^{-3}$ and the hydrogens exist neither as H_2O nor H_2 molecules, but mainly form $-\text{OH}$ bonds. In such a case, it is considered that the H is ionized to H^+ and should work as a shallow donor by releasing a free electron as suggested by first-principles calculations.⁴

Figures 2a and 2b show hydrogen SIMS (H-SIMS) depth profiles and electrical properties (i.e., electrical conductivity (σ), N_e and Hall mobility (μ_{Hall})) for the a-IGZO films as-deposited and annealed in a 5%- H_2 /95%- N_2 atmosphere at annealing temperatures of $T_{\text{ann}} = 100\text{--}400^\circ\text{C}$. Although the as-deposited film contained H of $\sim 10^{21} \text{ cm}^{-3}$, the measured N_e was only $\sim 3 \times 10^{15} \text{ cm}^{-3}$, suggesting that the H were mostly inactive as an electron donor. It was found that a-IGZO can incorporate excess weakly-bonded oxygens as detected by TDS.⁵ Therefore, we consider that the hydrogens incorporated in the as-deposited films generate free electrons by forming

^zE-mail: nomura@lucid.msl.titech.ac.jp

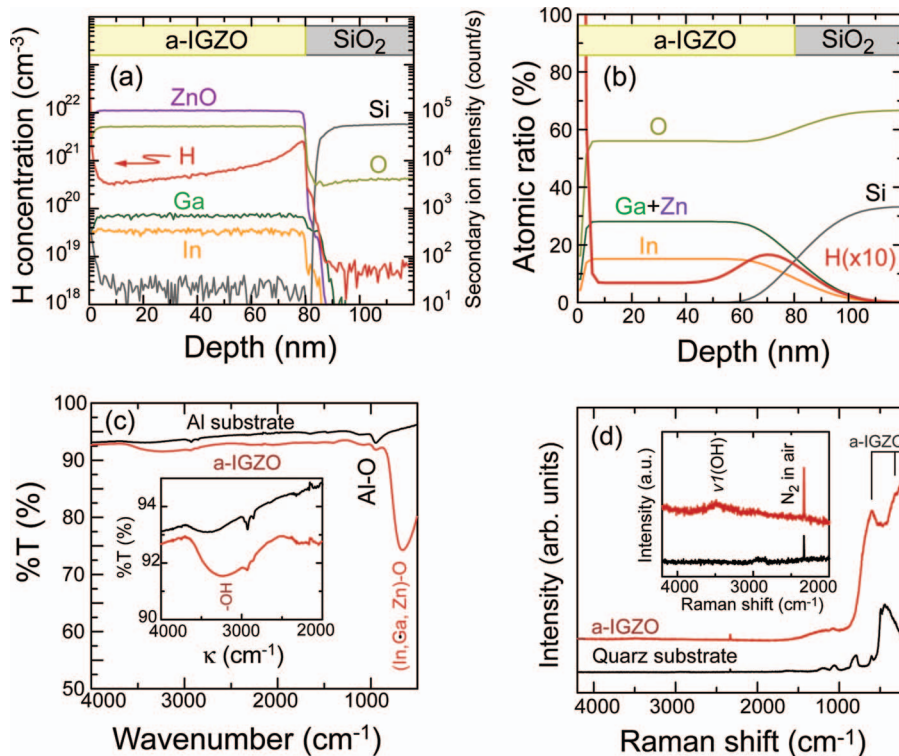


Figure 1. (a) SIMS and (b) RBF/HFS depth profiles for as-deposited a-IGZO films. (c) ATR-FTIR and (d) Raman spectra for the as-deposited films. Insets show magnified views. Aluminum metal and anhydrous silica glass substrates were used for ATR-FTIR and Raman measurements, respectively.

–OH bonds, but the released free electrons are compensated by the excess oxygens because an O atom tends to capture electrons to form an O^-/O^{2-} ion.

On the other hand, upon post-deposition annealing in the H_2/N_2 gas, the N_e steeply increased to $>10^{18} \text{ cm}^{-3}$ even by the 100°C annealing and further increased to $\sim 8 \times 10^{19} \text{ cm}^{-3}$ as T_{ann} was raised to 400°C , but the H concentration was nearly unchanged. The TDS measurements of as-deposited films revealed that desorption of oxygen-related species such as H_2O and O_2 were not detected at temperatures below 120°C .⁶ Therefore, the steep increase of N_e by the 100°C annealing cannot be explained by carrier generation via the formation of oxygen deficiencies, and it should be attributed to the desorption of surface oxygens and/or the reduction of deep traps near the valence band maximum, which was observed by hard X-ray photoemission spectroscopy.⁸

On the other hand, the increase of N_e in the higher temperature region ($120\text{--}300^\circ\text{C}$) was mainly attributed to the desorption of the O- and H-related species as detected by TDS because, in particular, the desorption curve of H_2O is similar to the variation of electrical conductivity.⁶ The saturation behavior at $>300^\circ\text{C}$ would be related to a doping limit under annealing conditions used in this study (note

that $N_e > 10^{20} \text{ cm}^{-3}$ have not been obtained by conventional annealing methods and only ion implantation succeeded).

Figures 3a and 3b show the ^2D and ^1H depth profiles for the films annealed at $100\text{--}400^\circ\text{C}$ in a 5%- D_2 /95%- N_2 gas. It was found that $>10^{18} \text{ cm}^{-3}$ of ^2D diffuses into the a-IGZO film at the depth of 10 nm from the surface even at the low temperature of 100°C . Figures 3c and 3d summarize the [^2D] and [^1H] (the brackets indicate concentrations) at the depth of 60 nm from the surface. Total contents (C_{tot}), i.e., the sum of [^1H] + [^2D], are also plotted. It shows that C_{tot} is nearly constant ($C_{\text{tot}} = 0.7\text{--}1.5 \times 10^{21} \text{ cm}^{-3}$) in the T_{ann} range $100\text{--}400^\circ\text{C}$, which is consistent with the result in Fig. 2a. On the other hand, most of the internal ^1H ($> 80\%$) were replaced by ^2D after the high T_{ann} at 400°C (Fig. 3d). The diffusion coefficients (D_{dif}) were evaluated from least-squares fitting of the data to the complementary error function (*erfc*), $C(x, t) = C_0 \text{erfc}(x D_{\text{dif}} t_D / 2)$, where C_0 is the surface concentration, x is the depth from the surface, and t_D is the diffusion time. The fitting results for in-/out-diffusions of ^2D and ^1H are also shown in Figs. 3a and 3b, which agree well with the SIMS data. The obtained D_{dif} for the in-diffusion of ^2D at 200°C is $2.6 \times 10^{-15} \text{ cm}^2 \text{ s}^{-1}$, which is much smaller than those in SiO_2 ($\gg 10^{-9} \text{ cm}^2 \text{ s}^{-1}$),⁹ and single-crystal ZnO ($\sim 10^{-10} \text{ cm}^2 \text{ s}^{-1}$) and

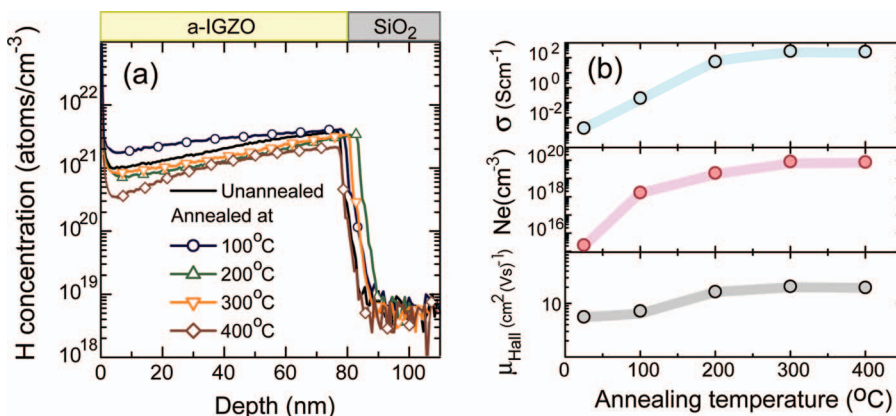


Figure 2. Variation of (a) hydrogen SIMS depth profiles and (b) electrical properties (σ , μ_{Hall} , and N_e) for a-IGZO films as-deposited and annealed in 5%- H_2 /95%- N_2 at $100\text{--}400^\circ\text{C}$ for 1 hour.

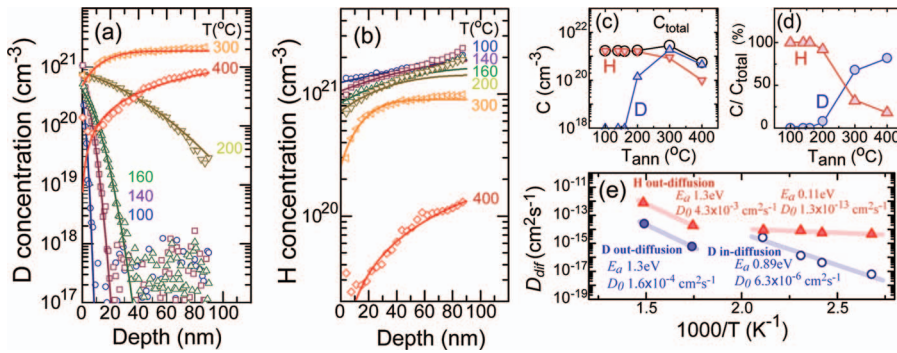


Figure 3. SIMS depth profiles (symbols) and fitting curves (solid lines) for (a) ^2D and (b) ^1H in a-IGZO film annealed at 100–400°C. (c) Variation of $[\text{}^2\text{D}]$ (blue triangles), $[\text{}^1\text{H}]$ (red triangles) at the depth of 60 nm from the surface and their sum ($C_{\text{total}} = [\text{}^2\text{D}] + [\text{}^1\text{H}]$, open circles) as a function of annealing temperature. (d) Variation of relative contents for ^2D and ^1H as a function of annealing temperature. (e) Arrhenius plots of diffusion coefficients for in-diffusion (blue open circles) and out-diffusion (blue closed circles) of ^2D and out-diffusion (red closed triangles) of ^1H .

poly-crystalline ZnO ($\sim 10^{-11} \text{ cm}^2\text{s}^{-1}$).^{10,11} It should be noted that hydrogens diffuse for $>30 \text{ nm}$ (measured at $[\text{H}] = 10^{18} \text{ cm}^{-3}$, which is a typical induced carrier concentration in a channel of TFT) even at 160°C and for $>200 \text{ nm}$ at 200°C ($[\text{H}] \gg 10^{19} \text{ cm}^{-3}$), being consistent with the previous result that N_e is increased by 200°C hydrogen annealing.

Figure 3e shows the Arrhenius plots of the obtained D_{diff} for the in-/out-diffusions of ^2D and ^1H . For the in-diffusion of ^2D (the blue open circles), the data follows well the Arrhenius relation $D(T) = D_0 \exp(-E_a/kT)$, where D_0 is the diffusion prefactor, E_a is the apparent activation energy, k is the Boltzmann constant and T is the annealing temperature. The obtained $E_a = 0.89 \text{ eV}$ is comparable to the E_a values reported for hydrogen diffusion in ZnO (1.12–0.91 eV). However, the D_0 of $6.3 \times 10^{-6} \text{ cm}^2\text{s}^{-1}$ differs largely from that in ZnO ($\sim 10^{-2} \text{ cm}^2\text{s}^{-1}$). These results indicate that the diffusive migration of H in a-IGZO is explained by hopping similar to other oxides, but the density of the hopping sites would be much lower due to the existence of the high-density H.

On the other hand, the D_{H} for the out-diffusion of ^1H (red triangles) shows complex behaviors with two temperature regions according to a small E_a of 0.11 eV at $\leq 200^\circ\text{C}$ and a large E_a of 1.3 eV at $\geq 300^\circ\text{C}$. The small E_a of 0.11 eV and fast D_{H} of $\sim 10^{-14} \text{ cm}^2\text{s}^{-1}$ in the low temperature region of $\leq 200^\circ\text{C}$ also suggest that a portion of the internal H in the as-deposited a-IGZO film diffuses out even at the low temperature, and would exist as weakly-bonded hydrogens. First-principles calculations showed the bonding energies of O–H bonds depend largely on the coordination structure of the O ion, which would cause the weakly-bonded hydrogen that can diffuse out at the low temperature.¹²

Figures 4a and 4b show the SIMS depth profiles of relative concentration of ^{18}O , which is defined as $C = I(^{18}\text{O}^-)/[I(^{16}\text{O}^-) + I(^{18}\text{O}^-)]$, where $I(^{18}\text{O})$ and $I(^{16}\text{O})$ are secondary ion intensity of ^{18}O and ^{16}O , respectively, and C_0 obtained from the least-squares fitting to *erfc* for the as-deposited films annealed at 100–400°C. These show that 0.01% (corresponds to 10^{18} cm^{-3}). Note that this density of defects

or free carriers is high enough to alter electrical properties of TFTs) of ^{16}O were replaced by ^{18}O after the annealing at 100°C in the 10 nm deep region of a-IGZO, which is extended to 20 nm at 400°C. The ^{18}O concentration near the film surface increases with rising the diffusion temperature, suggesting that surface migration and/or reaction control the oxygen diffusion in a-IGZO. The D_{diff} values are $2\text{--}4 \times 10^{-17} \text{ cm}^2\text{s}^{-1}$ for the films annealed at 100–400°C, which are two or more orders of magnitude faster than that in ZnO ($\sim 10^{-22} \text{ cm}^2\text{s}^{-1}$ for single-crystal and $\sim 10^{-19} \text{ cm}^2\text{s}^{-1}$ for epitaxial films at 400°C).¹³ However, the D_0 values are nearly temperature independent and provide very small E_a of $\sim 0.03 \text{ eV}$ and D_0 of $\sim 4.9 \times 10^{-17} \text{ cm}^2\text{s}^{-1}$ (Fig. 4c), which are much smaller than those for ZnO films ($E_a = 1.1\text{--}1.0 \text{ eV}$ and $D_0 \sim 2\text{--}3 \times 10^{-10} \text{ cm}^2\text{s}^{-1}$ in the temperature range of $T_{\text{meas}} = 730\text{--}1190^\circ\text{C}$) and SiO_2 ($E_a = 1.3 \text{ eV}$ and $D_0 \sim 2 \times 10^{-9} \text{ cm}^2\text{s}^{-1}$ in $T_{\text{meas}} = 850\text{--}1250^\circ\text{C}$).¹⁴ The E_a became large in the 400°C-thermally annealed films in oxygen containing atmosphere and are ~ 0.17 and $\sim 0.11 \text{ eV}$ for 400°C-wet and dry oxygen annealed films, respectively. However, they are still much smaller than those for oxygen diffusion in ZnO and SiO_2 . Several mechanisms have been proposed for oxygen migration in oxides, including a hopping mechanism between vacancy/interstitial sites.¹⁵ However, the obtained E_a were too small to understand as the hopping mechanism. Therefore, we speculate at the present stage that the ‘large D_0 value even at 100°C and the small E_a ’ reflects the migration of weakly-bonded oxygens and/or atomic oxygens generated by O_2 dissociation at the film surface, which are chemically active due to the presence of high density oxygen vacancy,¹⁶ via the void structures.¹⁷

In conclusion, we found that as-deposited a-IGZO thin films contained high-density hydrogens at $>10^{20} \text{ cm}^{-3}$, which form M–OH bonds. It is accepted that the hydrogen is ionized and releases a free electron in many oxide semiconductors such as ZnO; however, in a-IGZO films, most of the electrons are compensated by excess oxygens in the as-deposited states, keeping the low free electron density of $N_e \sim 10^{15} \text{ cm}^{-3}$. The D_{diff} of hydrogen is $\sim 2.6 \times 10^{-15} \text{ cm}^2\text{s}^{-1}$ at 200°C, which is two orders of magnitude larger than that of oxygen

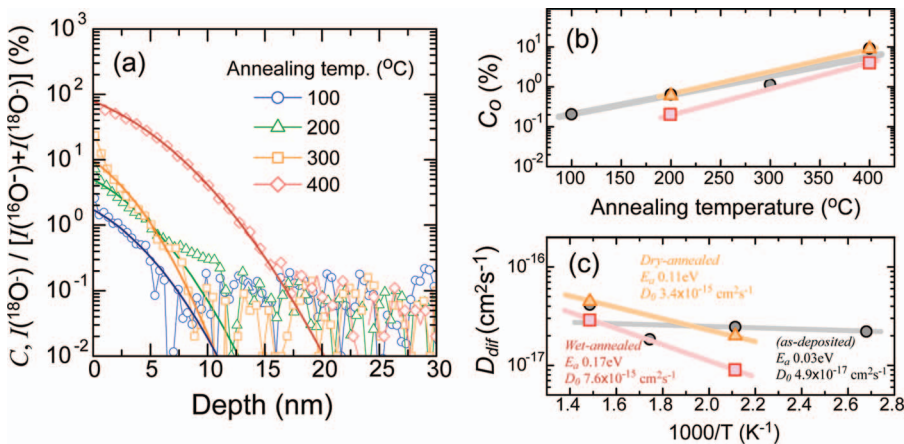


Figure 4. (a) ^{18}O depth profile (symbols) and fitting curves (solid lines) for as-deposited a-IGZO films annealed at 100–400°C for 1 hour. (b) Variation of C_0 as a function of annealing temperature. (c) Diffusion coefficient as a function of reciprocal temperature. For comparison, those for 400°C-wet/dry oxygen annealed films⁶ are also shown.

($3 \times 10^{-17} \text{ cm}^2\text{s}^{-1}$) but several orders of magnitude smaller than that of ZnO, and is attributed to low-density diffusion hopping sites due to the existence of the high-density hydrogens. If we take the hydrogen D_{dif} value of $2.6 \times 10^{-15} \text{ cm}^2\text{s}^{-1}$, the mobility is estimated to be $\mu \sim 10^{-13} \text{ cm}^2(\text{Vs})^{-1}$ using the Einstein's relation $D_{\text{dif}} = (kT/e)\mu$ and the RT energy of $kT = 0.026 \text{ eV}$. This value is more than 10 orders of magnitude larger than the obtained mobility of positive charge for negative bias light illumination (NBI) instability test ($\sim 0.01 \text{ cm}^2\text{s}^{-1}$),¹⁸ suggesting that proton capture is not a dominant origin of the NBI instability under usual bias conditions.

Acknowledgments

This work was supported by the Funding Program for World-Leading Innovative R&D on Science and Technology (FIRST) of Japan Society for the Promotion of Science (JSPS).

References

1. K. Nomura, H. Ohta, A. Takagi, T. Kamiya, M. Hirano, and H. Hosono, *Nature*, **432**, 488 (2004).
2. T. Kamiya, K. Nomura, and H. Hosono, *Sci. Technol. Adv. Mater.*, **11**, 044305 (2010).
3. C. G. Van de Walle, *Phys. Rev. Lett.*, **85**, 1012 (2000).
4. T. Kamiya, K. Nomura, and H. Hosono, *Phys. Status Solidi A*, **206**, 860 (2009).
5. K. Ide, Y. Kikuchi, K. Nomura, M. Kimura, T. Kamiya, and H. Hosono, *Appl. Phys. Lett.*, **99**, 039507 (2011).
6. K. Nomura, T. Kamiya, H. Ohta, M. Hirano, and H. Hosono, *Appl. Phys. Lett.*, **93**, 192107 (2008).
7. R. L. DeRosa, P. A. Schader, and J. E. Shelby, *J. Non-Cryst. Solids*, **331**, 32 (2003).
8. K. Nomura, T. Kamiya, H. Yanagi, E. Ikenaga, K. Yang, K. Kobayashi, M. Hirano, and H. Hosono, *Appl. Phys. Lett.*, **92**, 202117 (2008).
9. D. Fink, J. Krauser, D. Nagengast, T. A. Murphy, J. Erxmeier, L. Palmetshofer, D. Briunig, and A. Weidinger, *Appl. Phys. A*, **61**, 381 (1995).
10. D. G. Thomas and J. J. Lander, *J. Chem. Phys.*, **25**, 1136 (1956).
11. N. H. Nickel, *Phys. Rev. B*, **75**, 035212 (2007).
12. T. Kamiya, K. Nomura, and H. Hosono, *Phys. Status Solidi A*, **207**, 1698 (2010).
13. H. Ryoken, I. Sakaguchi, N. Ohashi, T. Sekiguchi, S. Hishita, and H. Haneda, *J. Mater. Res.*, **20**, 2866 (2005).
14. E. L. Williams, *J. Amer. Ceram. Soc.*, **48**, 190 (1965).
15. A. F. Kohan, G. Ceder, D. Morgan, and C. G. Van de Walle, *Phys. Rev. B*, **61**, 15019 (2000).
16. K. Nomura, T. Kamiya, E. Ikenaga, H. Yanagi, K. Kobayashi, and H. Hosono, *J. Appl. Phys.*, **109**, 073726 (2011).
17. K. Nomura, T. Kamiya, H. Ohta, T. Uruga, M. Hirano, and H. Hosono, *Phys. Rev. B*, **75**, 035212 (2007).
18. K. Nomura, T. Kamiya, and H. Hosono, *Appl. Phys. Lett.*, **99**, 053505 (2011).